MODELING WOOD STRANDS AS MULTI-LAYER COMPOSITES: BENDING AND TENSION LOADS

Daniel P. Hindman

Assistant Professor
Department of Wood Science and Forest Products
Virginia Polytechnic Institute and State University
1650 Ramble Road
Blacksburg, VA 24061

and

Jong Nam Lee

Research Scientist
Department of Wood Science and Forest Products
Virginia Polytechnic Institute and State University
1650 Ramble Road
Blacksburg, VA 24061

ABSTRACT

Wood strands are composed of distinct layers of earlywood and latewood material. Previous research has demonstrated that latewood mechanical properties may be two to three times greater than earlywood mechanical properties. However, wood composite modeling assumes strands are uniform, homogenous elements. This paper investigated the effect of considering wood strands as two-layer composites consisting of earlywood and latewood, or intra-ring, layers. Experimental measurement of the intra-ring properties of loblolly pine (*P. taeda*) provided inputs to finite element models using both solid layers and cellular layers to represent longitudinal tracheids. The models were compared with three different types of strands cut at various orientations (flatsawn, quartersawn, non-aligned cut) in both tension and bending loadings. The model prediction of strand stiffness greatly improved by considering the strands as 2-layer composites compared to homogenous sections. Further improvements of the prediction of stiffness were made from modeling cellular layers rather than solid layers. The rule of mixtures predictions of stiffness produced good agreement for the non-aligned strands in both tension and bending loading, but only good agreement in the tension loading for the flatsawn strand. Examining the stress distributions of the strands from the finite element model, the solid models showed distinct stress changes at the edges of the intra-ring layers, indicating stress concentrations at the boundaries of the intra-ring layers. The cellular models showed a much more gradual stress transition between the intra-ring layers, which is a more realistic scenario.

Keywords: Intra-ring properties, earlywood, latewood, mechanical properties.

INTRODUCTION

As more focus is given to smaller wood fiber sources, there is a lack of information about wood at the micro-scale level. The micro-scale level is defined as the range of 10^{-3} to 10^{-6} m, which compromises the anatomical formations of earlywood and latewood. A cursory review of wood anatomy will demonstrate the heterogeneity of cellular types, sizes, directional orientations and chemical complexity associated with wood materials. While this complexity may seem overwhelming, some of the most important anatomical features are the earlywood and latewood layers in the annular rings. The understanding of the interaction of the earlywood and latewood, or intra-ring, layers is important for the understanding of the micro-scale mechanical behavior of wood materials. The effects of considering the intra-ring layers in modeling the mechanical properties of wood strands have not been demonstrated previously.

Previous testing by researchers has demonstrated that the strength and stiffness of earlywood is two to three times less than latewood (Cramer et al. 2005). With changes in the wood material resource to include more juvenile wood, there is now a higher percentage of earlywood present compared to mature wood. Many plantation-grown and alternative wood species used for wood fiber production have a lower density and may contain greater percentages of earlywood (Larson et al. 2001). Therefore, the changes in earlywood and latewood percentages may lead to fundamental changes in wood materials which may affect wood composite production.

Modeling efforts provide us with a virtual material to observe mechanical behavior under different end-use conditions. Wood composite properties can be predicted from a variety of models which incorporate lay-up variables, uses of different adhesives and manufacturing variables. One important component in the production of composite materials is the prediction of mechanical properties based on the constituent individual strand or fiber properties. However, most of these models consider the wood fiber source to be represented by homogenous, uniform elements. The understanding of the earlywood and latewood properties of wood fiber sources will allow more refined modeling efforts in the prediction of composite properties. Gibson (2005) notes that wood can be described as a composite composed of two-dimensional cellular elements. Salmén (2004) states "a better understanding of the relationships between its [wood] macroscopic mechanical properties, fiber ultrastructure and properties of wood polymers is important."

LITERATURE REVIEW

Several authors have measured the strength and stiffness of wood fibers. Jayne (1959) measured the tensile strength and modulus of elasticity of pulped wood fibers from ten softwood species. Groom et al. (2002) and Mott et al. (2002) both tested single wood tracheids mechanically removed from loblolly pine samples. The tracheids were tested in a foliar frame system using a ball and socket arrangement. These two articles by Groom et al. (2002) and Mott et al. (2002) represent the latewood and earlywood, respectively, material property measurements. Cramer et al. (2005) used a broadband viscoelastic spectroscopy (BSV) device to measure the longitudinal modulus of elasticity and the longitudinal-radial shear modulus of loblolly pine samples. The BSV is capable of applying both bending and torsion loads for mechanical property evaluation. Other authors have tested the off-axis properties at the micro-scale level, including Dumail and Salmén (2001), who tested the in-plane shear modulus and Farruggia and Perré (2000) who tested the transverse elastic properties.

Table 1 demonstrates the differences between the strength and stiffness of earlywood and latewood. For the tensile modulus, the latewood values were 2.38 to 1.33 times greater than the earlywood values. For the tensile strength, the latewood values were 2.72 to 1.72 times greater than the earlywood values. Previous research has demonstrated great differences between the earlywood and latewood stiffness and strength. Earlywood and latewood demonstrate different strength and stiffness behavior which should be modeled as distinct layers.

TABLE 1. *Earlywood and latewood material properties from previous studies.*

Material	Tensile modulus, GPa		Tensile strength, MPa		Reference
	Earlywood	Latewood	Earlywood	Latewood	
White spruce (*Picea glauca*)	25.2	35.1	523	569	Jayne (1959)
Douglas fir (*Pseudotsuga menziesii*)	17.8	42.6	344	951	Jayne (1959)
Loblolly pine (*Pinus taeda*) tracheids	N/A	19.7	N/A	1040	Groom et al. (2002)
Loblolly pine (*P. taeda*) tracheids	14.8	N/A	604	N/A	Mott et al. (2002)
Loblolly pine (*P. taeda*)	4.34	9.88	N/A	N/A	Cramer et al. (2005)

There has been no previously published work on the modeling of wood strands composed of intra-ring layers. However, some previous studies have modeled wood composites or wood fiber response and these models can serve as guides for intra-ring property modeling. Triche and Hunt (1993) developed a model for the prediction of tensile strength of parallel aligned composites using the finite element method. Hepworth and Vincent (1998) modeled xylem tissue of tobacco (*Nicotiana tabacum 'Samsun'*) using a series of fibers embedded in a pliable matrix. Wang and Lam (1998) developed a nonlinear finite element model for multiple strand layers that incorporated off-axis strand orientation and gaps within the composite.

The goal of this research was to examine the effect of intra-ring properties upon the strength and stiffness of wood strands subjected to bending and tension loadings. Two different models were constructed to simulate the mechanical behavior of a wood strand—a homogenous model and a model with intra-ring variation. Sections of earlywood and latewood material were sampled to provide tensile and bending input values for the models. The model results were compared to a series of three strands representing different intra-ring orientations. The stiffness properties of the models were compared with experimental test results for verification.

This modeling described the expected properties of strands based upon mechanical properties and earlywood and latewood layer sizes. This modeling may be important for prediction of the effect of substituting different wood species having different ultrastructural characteristics and juvenile wood.

MATERIALS

All samples were prepared from loblolly pine (P. *taeda*) obtained from a local source. Logs were cut into wood blocks measuring 15.2 cm by 15.2 cm by 2.54 cm and then soaked in water to reduce flaking damage. Straight-grained blocks were randomly selected to produce earlywood and latewood samples. Strands were produced 15.2 cm long, 2.54 cm wide, and 0.68 cm thick using a disc flaker located in the Wood-Based Composites Laboratory at the Brooks Forest Products Center at Virginia Tech. After flaking, strands with excessive damage were culled. All strands were dried in an oven at 110 degrees C and 0% RH. The strands were stored in resealable plastic bags stored inside a larger plastic container.

EXPERIMENTAL TESTING

Testing of earlywood and latewood samples

Samples of earlywood and latewood were subjected to both tension and bending testing. A Minimat 2000 Miniature Materials Tester from Rheometric Scientific, Inc. was used for all earlywood and latewood material evaluation. At present, there is no standard for the testing of strands or small wood materials. However, ASTM D 143 (ASTM 2004) was used as a guide to establish loading rates and appropriate test procedures. Figure 1 shows the testing of tension and bending samples using the Minimat tester. The Minimat tester contains an integral 200 N load cell and uses the Minimat data acquisition software to collect all load and position data.

Tension testing used samples that were approximately 60 mm long and 0.66 mm thick. Earlywood samples were approximately 4.58 mm wide, while latewood samples were 3.3 mm wide. A gage length of approximately 40 mm was used with the ends of the strand wrapped in sandpaper and placed in the grooved tension grips to prevent the specimen from slipping. A testing speed of 0.127 mm/min was applied. Load and crosshead position were measured until failure of the specimen occurred. From the ultimate load and the load-deflection curve, the tensile strength and tensile modulus were calculated.

Bending tests used samples that were approximately 33.0 mm long, 11.0 mm wide, and 0.68 mm thick. The tests were performed flatwise with a three-point bending fixture. Two supports were located 18.11 mm apart with a load point at the midspan of the beam. The maximum load
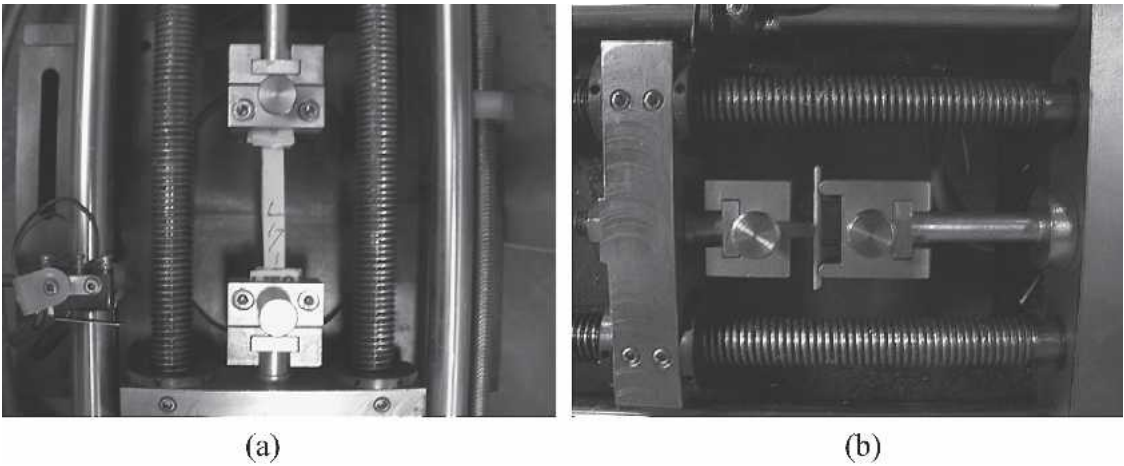
F<small>IG</small>. 1.   Testing of earlywood and latewood samples using minimat, (a) tension testing, (b) bending testing.

and load-deflection curve were used to calculate the MOR and bending modulus.

Experimental testing of strands

In order to verify the models developed for wood strands considering earlywood and latewood as different layers, three distinct cutting patterns were analyzed. Figure 2 shows the three strands used as well as a representation of each strand within the radial alignment of a tree. Strand A was cut in the LR plane producing flatsawn strands. Strand B was cut with a small angle to the LT plane producing quartersawn strands. Strand C was cut with at an angle to both the LR and LT planes, which represents non-aligned cut strands.

Table 2 shows the characteristics of the three strand types used, including the average number
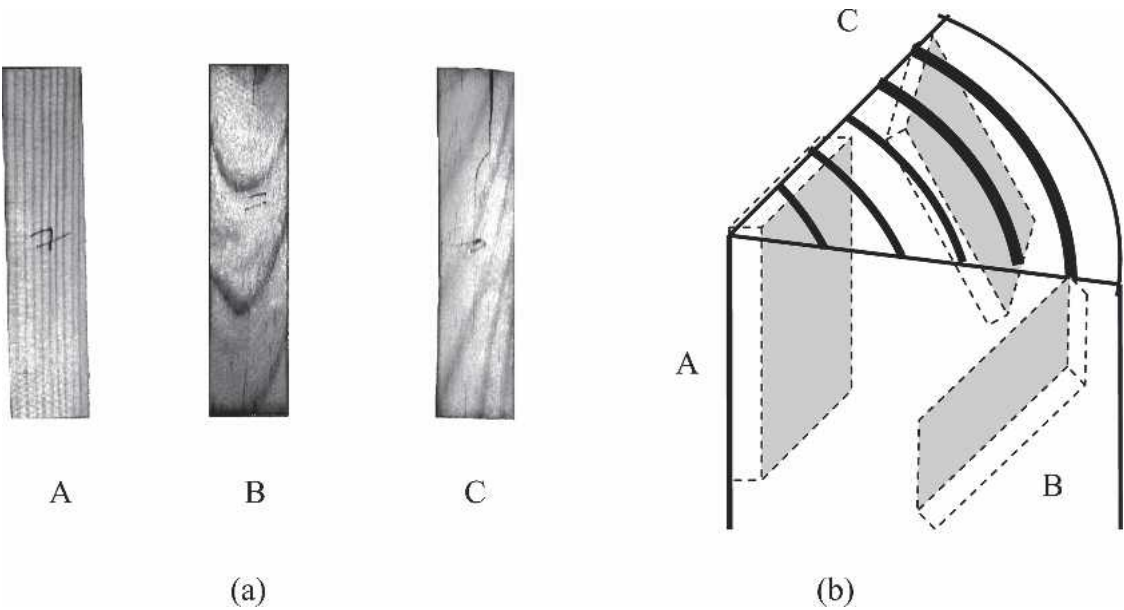

F<small>IG</small>. 2.   Full-sized strands, (a) three types of strands, (b) relative position within a log.

TABLE 2. *Average properties of three strand types used for model verification.*

Strand type	Strand description	No. LW bands	Width of LW bands (mm)	Slope of rings (°)	Volume fraction of LW (%)
A	Quartersawn	9.4	1.22	1.57	55.4
B	Flatsawn	5.6	2.00	7.21	21.2
C	General cut	3.2	2.51	8.75	25.9
Mean		6.0	1.91	7.25	34.2

of latewood bands, width of latewood bands, slope of rings, and volume fractions of latewood observed for full-size strands generated from the flaker (2.54 cm wide). Tension and bending tests were conducted following the same procedure described for the earlywood and latewood samples. Tension samples were 60 mm long, 5.07 mm wide, and 0.66 mm thick. Bending specimens were the same size used in the earlywood and latewood sample testing.

FINITE ELEMENT MODEL DEVELOPMENT

Several finite element models were created to predict the stiffness of the wood strands based upon the constituent properties of the earlywood and latewood experimental stiffness results for tension and bending. The finite element models were constructed to examine the differences between considering the wood strand as a homogenous material or a composite of earlywood and latewood. Two different kinds of model were used to simulate the strands—a solid model and a cellular model. The cellular model is thought to more closely simulate the softwood tracheids, while the solid model represents a simpler finite element construction. Finite element modeling used the ANSYS v.9 program for all analysis. Figure 3 shows the mesh distribution of the finite element models used. These models show similar earlywood and latewood distribution compared to the three strands from Fig. 2.

All finite element models used the following assumptions:

1. Each wood strand is uniform in thickness with rectangular surfaces. All sides were perpendicular to each other and to the faces of the strand.
2. The mechanical behavior of multiple layers

of EW and LW cells was represented by five layers of different properties.
3. Wood cells were assumed to act as either solid elements or shells representing cells.
4. Only longitudinal tracheids were considered in this modeling.
5. Bonding between wood cells was assumed rigid with no slippage.
6. Cross-sections of the constituent elements remain plain and normal to the surface of the strand under bending loads.
7. All elements were assumed to be linearly elastic.
8. Latewood cell walls were assumed to be twice as thick as earlywood cell walls.
9. Longitudinal stiffness properties were measured experimentally while other elastic constants were generated from elastic constant ratios (Bodig and Jayne 1982).

For the solid modeling, three-dimensional 8-node hexahedral brick (Solid 45) elements were used. The number of elements used in the solid models was between 9147 and 36,000 tetrahedral elements depending upon the geometric complexity of the strand orientation. For the cellular modeling, a three-dimensional 10-node tetrahedral element (Solid 187) was used. The number of elements used in the cellular models was between 10,800 and 25,930 elements.

Figure 4 shows the loading and boundary conditions used for the tension and bending load cases. A tension force was applied uniformly to one end of the strand, while the other end was restrained by pin connections. For the bending loading, a triangular distribution of load was applied to simulate a case of pure bending stress. Given the large aspect ratio from the bending testing (a/h = 13.3), the case of pure bending should dominate the stress.
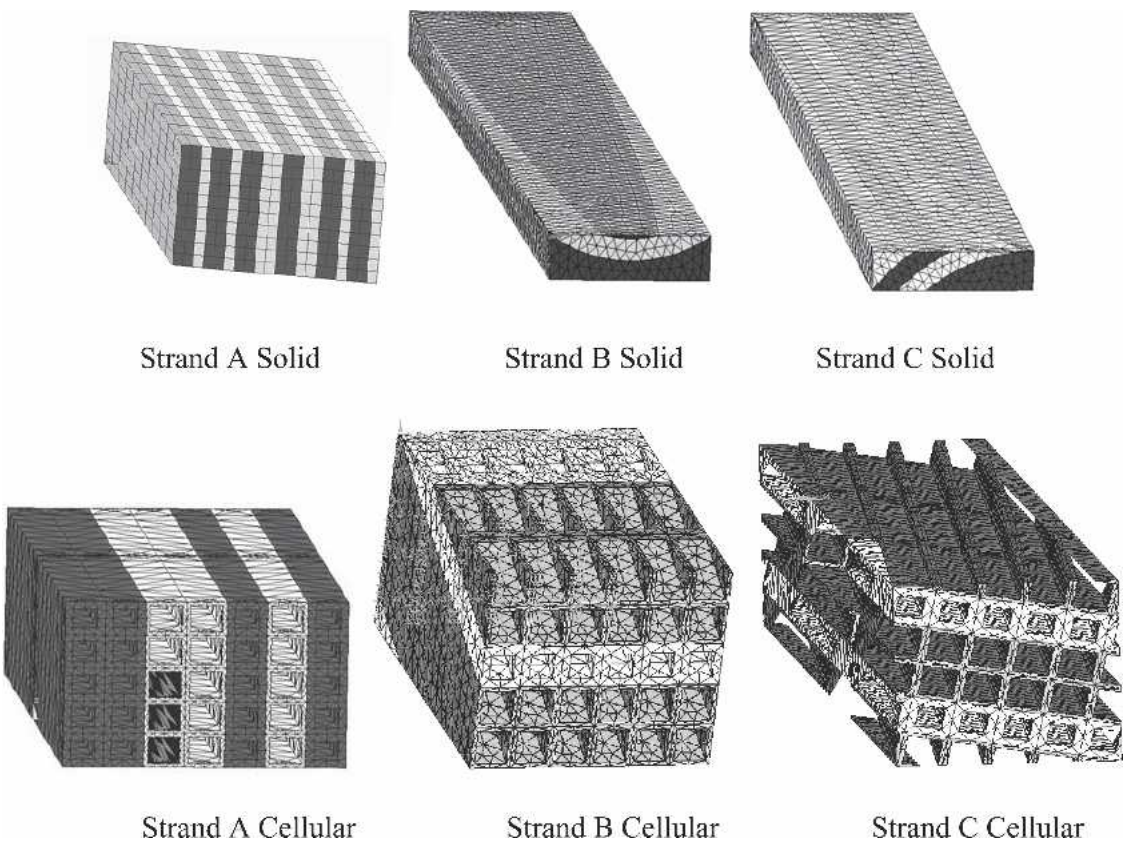
FIG. 3.   Finite element meshes generated for solution of strand types.

RULE OF MIXTURES ANALYTICAL MODEL

The rule of mixtures (R of M) model predicted the stiffness of the strands for comparison to experimental results. This model ignores the ring curvature and considers the cross-section of the strand to be uniform throughout assuming a constant earlywood and latewood percentage.
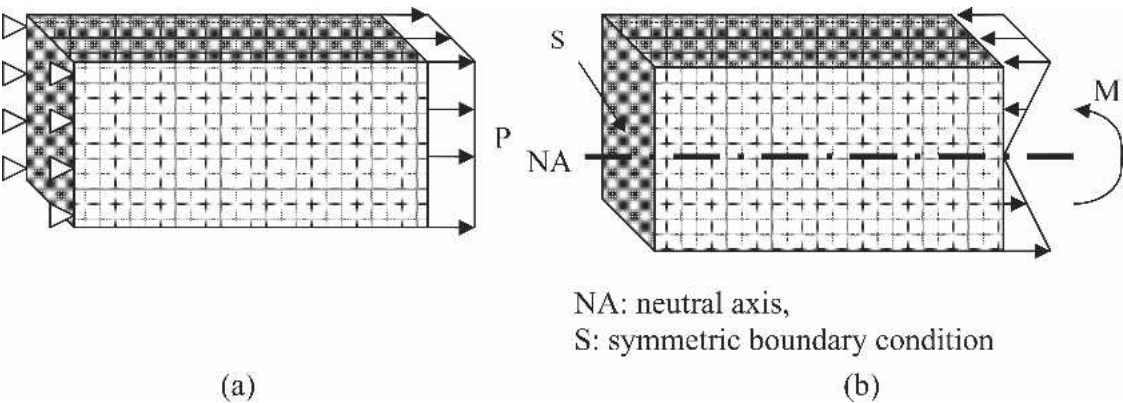

FIG. 4.   Loading conditions for (a) tension and (b) bending for all finite element modeling.

Most composite textbooks such as Jones (1999) discuss the rule of mixtures. This is a simple yet powerful model of composites where the composite modulus of elasticity is calculated by summing the volume fractions of the different constituent materials multiplied by their individual moduli of elasticity. Equation (1) shows the modulus of elasticity for the rule of mixtures model, the volume fraction and modulus of elasticity of earlywood and latewood.

$$E_{RofM} = \frac{1}{\dfrac{V_{EW}}{E_{EW}} + \dfrac{V_{LW}}{E_{LW}}} \tag{1}$$

where

E_{RofM} = modulus of elasticity from the rule of mixtures model

V_{EW} = volume fraction of earlywood in strand (%)

V_{LW} = volume fraction of latewood in strand (%)

E_{EW} = modulus of elasticity of earlywood

E_{LW} = modulus of elasticity of latewood

RESULTS AND DISCUSSION

Experimental testing results

Table 3 shows the specific gravity and results of experimental testing using the Minimat testing device. Specific gravity values for the earlywood fibers from tension and bending testing were 0.372 and 0.283, respectively, while the specific gravity for the latewood fibers were 0.714 and 0.677, respectively. The ratio of late-

wood to earlywood tensile modulus was 2.35:1 and the ratio of the tensile strength was 1.77:1. These ratios are similar to the previous research measured by Groom et al. (2002), Mott et al. (2002), and Cramer et al. (2005). The ratio of latewood to earlywood bending modulus was 3.41:1 and the ratio of the bending strength was 2.50:1. Megraw et al. (1999) reported that the average ratio of LW/EW in bending modulus was 2.3 with a COV of 51%. The COVs from the latewood samples are much higher than the COVs from the earlywood samples. During testing, the latewood showed higher fragility, which was also noted by Farruggia and Perré (2000).

From the three composite strands displayed in Table 3, the strands demonstrate different trends for the tensile and bending testing results. Strand A had the greatest tensile properties, followed by strand C and then strand B. For the bending properties, strand A had the greatest bending properties followed by strand B and then strand C. The difference between the order of bending and tensile properties may be explained by strand B containing the smallest volume fraction of latewood (Table 2). Strand C had the highest slope of rings with the smallest number of LW bands.

Modeling results

Table 4 shows the FEM and rule of mixtures model results compared to the average measured strand stiffness. The homogenous model values of the tension stiffness for strand A were 7.22% and 8.62% different for the solid and cellular models, respectively. However, the homogenous

TABLE 3. *Tensile and bending strength and stiffness of all strands tested.*

Property	Tensile properties			Bending properties		
	Specific gravity, (COV)	Modulus, E_L, GPa (COV)	Strength, MPa (COV)	Specific gravity, (COV)	Modulus, E_L, GPa (COV)	Strength, MPa (COV)
Earlywood	0.372 (16.2%)	2.71 (27.6%)	27.5 (30.4%)	0.283 (11.3%)	1.92 (23.4%)	35.3 (18.6%)
Latewood	0.714 (11.4%)	6.38 (55.1%)	48.8 (36.2%)	0.677 (11.5%)	6.54 (33.1%)	88.3 (25.4%)
A	0.456 (17.4%)	4.91 (21.1%)	43.3 (19.1%)	0.552 (21.5%)	5.78 (36.2%)	89.2 (27.6%)
B	0.412 (12.9%)	2.86 (29.8%)	13.5 (54.6%)	0.477 (16.5%)	4.71 (30.8%)	66.8 (24.8%)
C	0.415 (27.7%)	4.10 (16.5%)	22.7 (28.8%)	0.547 (10.2%)	3.42 (84.2%)	50.5 (61.6%)

TABLE 4. *Comparison of model results to experimental stiffness measurements.*

Model	Strand type	Tensile properties		Bending properties	
		Modulus, GPa	% Difference[1]	Modulus, MPa	% Difference[1]
Homogenous FEM model					
Solid model	A	5.268	7.22%	6.449	11.7%
	B		84.4%		36.8%
	C		28.6%		88.7%
Cellular model	A	5.337	8.62%	6.663	14.7%
	B		86.8%		40.5%
	C		30.3%		90.8%
Layered FEM model					
Solid model	A	4.378	−10.9%	6.255	8.30%
	B	3.023	5.83%	4.553	33.2%
	C	6.376	55.55%	5.279	12.0%
Cellular model	A	4.774	−1.70%	6.138	6.27%
	B	3.181	11.4%	4.116	20.4%
	C	4.813	17.5%	5.054	7.21%
Rule of mixtures	A	4.743	3.40%	4.479	22.5%
	B	3.489	−22.0%	2.899	38.4%
	C	3.661	10.7%	3.116	8.87%

[1] % Difference = (Model-Experimental)/Experimental × 100%.

model did not predict the strand B or strand C values well. Strand A was a flatsawn strand which had the highest number of earlywood and latewood layers. Looking at Fig. 3, the cross-section of strand A was uniform along the entire length. The ring orientation of the other strands led to discontinuous distributions of the earlywood and latewood throughout the cross-section (the most noticeable example was strand C in Fig. 3 with the large earlywood band at the bottom of the picture).

One of the general trends from Table 4 is the difference in the prediction of tension and bending stiffness. The percent difference terms for the homogenous model followed the same trends as the magnitude of the tensile and bending stiffness in Table 3. For tension, strand A was predicted best, followed by strand C, and then strand B. For bending strand A was predicted best, followed by strand B and then strand C. The reverse trend occurred in the layered models. For the tension models, strand B was always predicted better than strand C. For the bending models, strand C was always predicted better than strand B. The difference in model predictions was believed to be connected to the position of earlywood and latewood layers with the varying stress field caused by bending.

Grotta et al. (2005) noted that there was a slight difference in stiffness and strength depending on the orientation of earlywood or latewood on the compression face of the specimen. Thus, the ring orientation of earlywood and latewood may provide different surfaces at the tension and compression faces causing the difference in prediction.

The layered FEM models improved the prediction capacity compared to the homogenous model for strands B and C. The use of the cellular model versus the solid model improved the predictions for all strand types except strand B in tension. All of the predicted stiffness values from the layered cellular model were 20.4% different or less from the experimental results, representing good agreement.

The rule of mixtures model demonstrated some agreement with the experimental results. For the tensile stiffness, strands A and C predictions were both less than 10.7% different. Strand B was not predicted well in either tension or bending. In bending, strand C was predicted well at 8.87% difference, while strand A was not predicted well. The rule of mixtures predictions were most accurate for strand C, which represents a non aligned cut strand.
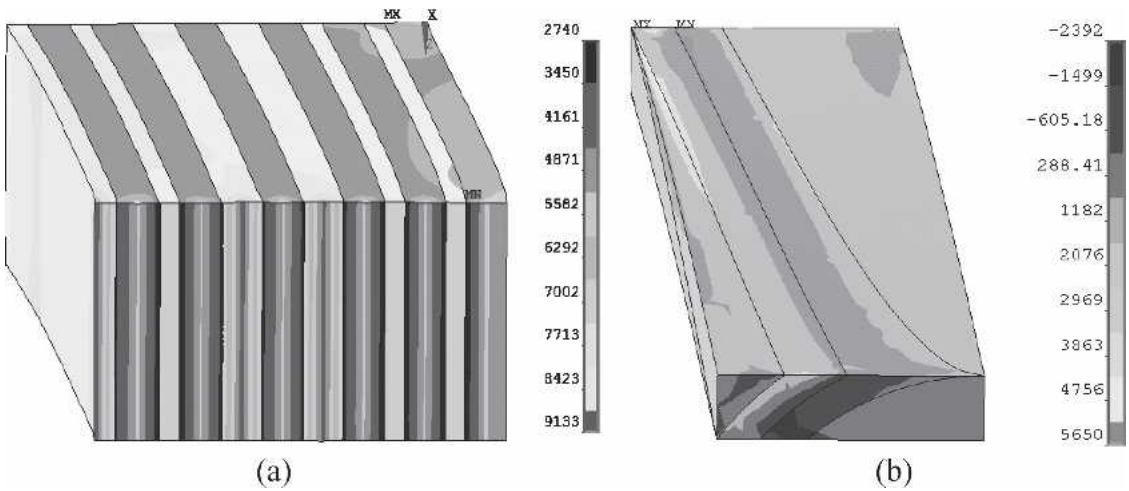
FIG. 5.   Stress values of solid layered models in tension, (a) strand A, (b) strand C.

Stress distribution of FEM models

While many images were generated from the tension and bending modeling of the different models, the following figures represent some selected images to illustrate the importance of considering wood strands as layered composites.

Figure 5 shows the solid layered models for strand A and C in tension. As shown in Fig. 4a, the pinned end is at the back of the images in Fig. 5 while the tension force was applied projecting out of the page. Strand A shows a striped pattern, where the earlywood layers were carrying a higher stress than the latewood layers due to the lower stiffness in the earlywood. Strand C

showed a stress pattern that is again higher in the earlywood layers than the latewood at the center of the strand. Note that the change in stress followed the ring orientation of the model.

Figure 6 showed the cellular layered models of strands A and B in tension loading. In strand A, the top surface had the same striped pattern as the solid layered model for strand A. However, there is a gradual change in the stress distribution throughout the depth of the strand. In Strand B, the change in stress is concentrated at the connection of the earlywood and latewood, with more stress being carried by the earlywood due to the lower stiffness properties. The cellular
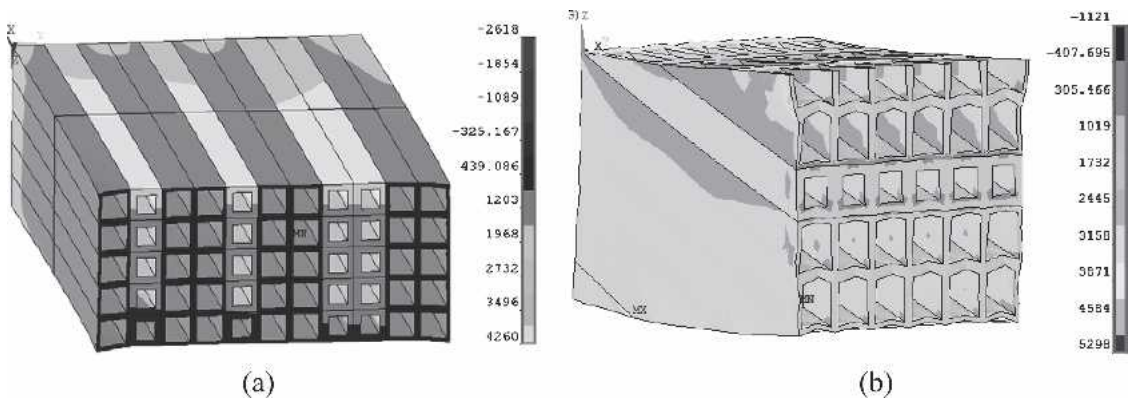

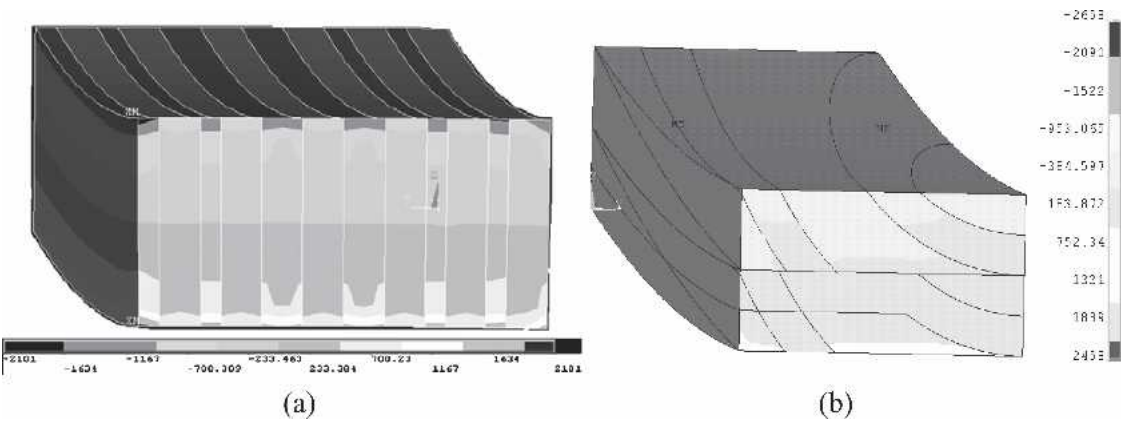FIG. 6.   FEM stress values of cellular layered models in tension, (a) strand A, (b) strand B.

FIG. 7.   FEM stress values of solid layered models in bending, (a) strand A, (b) strand C.

model demonstrated a more continuous stress trend between the intra-ring layers compared to the abrupt stress changes from solid modeling in Fig. 5a.

Figure 7 showed the solid layered models of strands A and C in bending loading. The loading was similar to Fig. 4b, with the symmetric condition applied at the back of the image and the triangular loading applied at the face of the element. The moment applied is causing curvature that depresses the center of the beam and raises the front and back edges. As in the tension load-

ing, strand A had a striped pattern between the earlywood and latewood bands. The change in color indicated that the earlywood contained stresses of greater magnitude than the latewood. Strand C had a more gradual transition of the stress across the face of the image. The narrower layers represented the latewood, which shows a transition point to the next color of stress further away from the neutral axis than the broader bands of earlywood.

Figure 8 showed the cellular layered models of strands B and C in bending. As in the tension
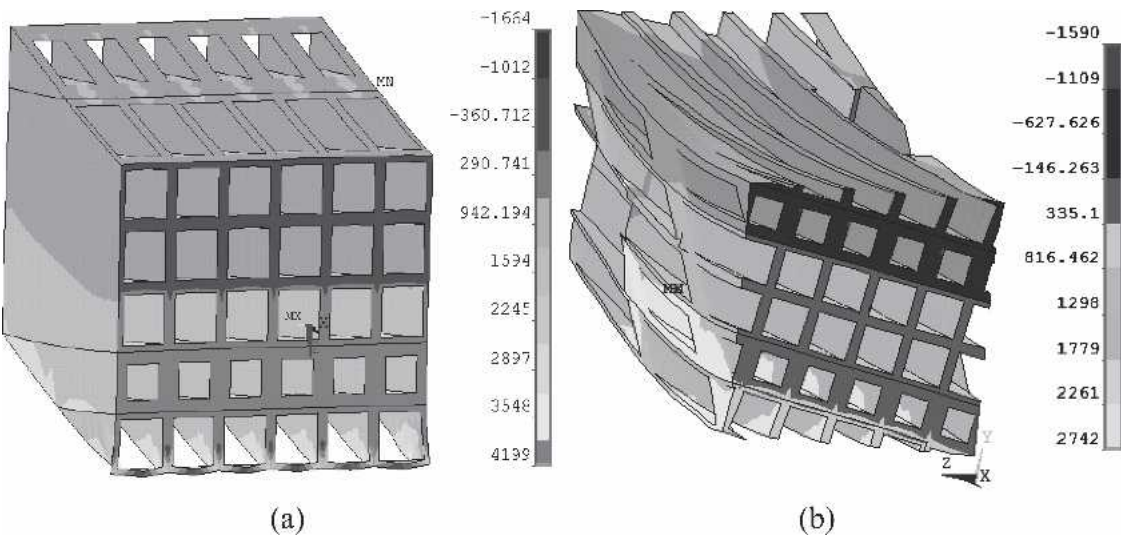

FIG. 8.   FEM stress values of cellular layered models in bending, (a) strand B, (b) strand C.

loading, the cellular modeling demonstrated a smoother transition of the stresses between the earlywood and latewood layers compared to the solid modeling. In strand B, there were places of high stress, such as the interface of the earlywood and latewood strands on top of the image and at the bottom of the image. For strand C, the stress transition was more uniform but contains some variation. There is a definite 'smudging' of the stress distribution since the intra-ring layers do not correspond to the principal directions of the stresses.

CONCLUSIONS

The purpose of this paper was to examine the effect of modeling wood strands as two-part composites consisting of earlywood and latewood materials. Experimental testing measured the strength and stiffness of earlywood and latewood samples in tension and bending. Finite element modeling and the rule of mixtures were used to develop models of the earlywood and latewood layers associated with wood strands. Models considering the different properties of earlywood and latewood layers provided improved agreement with experimental results compared to homogenous strand modeling The modeling of wood cells as cellular elements was a further improvement over consideration of the strands as solid elements. The rule of mixtures model provided good agreement in tension and bending for the nonaligned strand, yet only good agreement in tension for the flatsawn strand. Examination of the stress distribution confirms that cellular modeling demonstrates a more realistic case considering the stress concentrations at the boundaries of the intra-ring layers.

ACKNOWLEDGMENT

REFERENCES

ASTM. 2004. Standard test methods for small clear specimens of timber. ASTM D 143–94. Annual Book of ASTM Standards. Vol. 4.10. ASTM, West Conshohocken, PA. 800 pp.

BODIG, J., AND B. A. JAYNE. 1982. Mechanics of wood and wood composites. Kreiger Publishing Company, Malabar, Florida. 712 pp.

CRAMER, S., D. KRETSCHMANN, R. LAKES, AND T. SCHMIDT. 2005. Earlywood and latewood elastic properties of loblolly pine. Holzforschung 59:531–538.

DUMAIL, J.-F., AND L. SALMÉN. 2001. Intra-ring variations in the rolling shear modulus of spruce wood. Holzforschung 55(5):549–553.

FARRUGGIA, F., AND P. PERRÉ. 2000. Microscopic tensile tests in the transverse plane of earlywood and latewood parts of spruce. Wood Sci. Technol. 34:65–82.

GERE, J. M., AND S. TIMOSHENKO. 1997. Mechanics of materials. Fourth Edition. PWS Publishing Company, New York, NY. 912 pp.

GIBSON, L. J. 2005. Biomechanics of cellular solids. Biomechanics. 38:377–399.

GROOM, L., L. MOTT, AND S. SHALER. 2002. Mechanical properties of individual southern pine fibers. Part I. Determination and variability of stress-strain curves with respect to tree height and juvenility. Wood Fiber Sci. 34(1):14–27.

GROTTA, A. T., R. J. LEICHTI, B. L. GARTNER, AND G. R. JOHNSON. 2005. Effect of growth ring orientation and placement of earlywood and latewood on MOE and MOR of very small clear Douglas-fir beams. Wood Fiber Sci. 37(2):207–212.

HEPWORTH, D. G., AND J. F. V. VINCENT. 1998. Modeling the mechanical properties of xylem tissue from tobacco plants (*Nicotiana tabacum 'Samsun'*) by considering the importance of molecular and micromechanisms. Annals Botany 81:761–770.

JAYNE, B. A. 1959. Mechanical properties of wood fibers. Tappi 42(6):461–467.

JONES, R. M. 1999. Mechanics of composite materials. Second Edition. Taylor and Francis, Inc, Philadelphia, PA. 519 pp.

LARSON, P. R., D. E. KRETSCHMANN, A. CLARK III, and J. G. Isebrands. 2001. Formation and properties of juvenile wood in southern pines. FPL-GTR-129. USDA Forest Service. Madison, WI. 42 pp.

MEGRAW, R., D. BREMER, G. LEAF, AND J. ROERS. 1999. Stiffness in loblolly pine as a function of ring position and height, and its relationship to microfibril angle and specific gravity. Pages 341–349 *in* Nepveu, G., ed. Proc. IUFRO WP S5.01–04 Third Workshop on Connection Between Silviculture and Wood Quality through Modeling Approaches and Simulation Software, La Londe-les-

Maures, Sept. 1999, Publication Equipe de Recherches sur la Qualité de Bois 1992/2, Dec., INRA-Nancy, France.

MOTT, L., L. GROOM, AND S. SHALER. 2002. Mechanical properties of individual southern pine fibers. Part II. Comparison of earlywood and latewood fibers with respect to tree height and juvenility. Wood Fiber Sci. 34(2): 221–237.

SALMÉN, L. 2004. Micromechanical understanding of the cell-wall structure. C. R. Biologies 327:873–880.

TRICHE, M. H., AND M. O. HUNT. 1993. Modeling of parallel-aligned wood strand composites. Forest Prod. J. 43(11/12): 33–44.

WANG, Y.-T., AND F. LAM. 1998. Computational modeling of material failure for parallel-aligned strand based wood composites. Computational Materials Science 11:157–165.

ZOMBORI, B. G., F. A. KAMKE, AND L. T. WATSON. 2001. Simulation of the mat formation process. Wood Fiber Sci. 33(4):564–579.